3-1-2011

Reducing Redundancies in Reconfigurable Antenna Structures Using Graph Models

Chaouki T. Abdallah

Joseph Costantine

Sinan al-Saffar

Christos G. Christodoulou

Reducing Redundancies in Reconfigurable Antenna Structures Using Graph Models

Joseph Costantine, *Member, IEEE*, Sinan al-Saffar, *Member, IEEE*, Christos G. Christodoulou, *Fellow, IEEE*, and Chaouki T. Abdallah, *Senior Member, IEEE*

***Abstract*—We present an approach for reducing redundancies in the design of reconfigurable antenna structures using graph models. The basics of graph models, their rules, and how they can be applied in the design of switch-based reconfigurable antennas are introduced. Based on these rules, a methodology is developed and formulated to reduce the number of switches and parts in the antenna structure, without sacrificing the desired antenna functions. This approach not only optimizes the overall structure of the antenna but it also reduces cost and overall losses. Several examples are presented and discussed to demonstrate the validity of this new approach through simulations and measurements that present good agreement.**

***Index Terms*—Graph theory, reconfigurable antennas, redundancy, switches.**

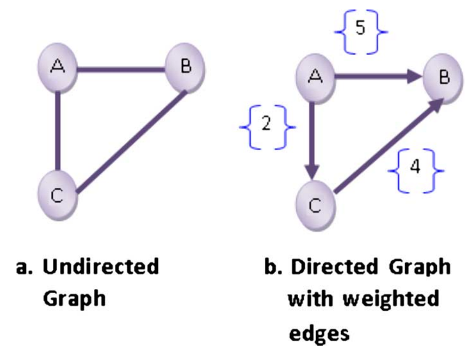

Fig. 1. a. An example of an undirected graph. b. An example of a directed graph with weighted edges.

I. Introduction

RECONFIGURABILITY, when used in the context of antennas, is the capacity to change an individual radiator's fundamental operating characteristics through electrical, mechanical, or other means [1]. The reconfiguration of such an antenna is achieved through an intentional redistribution of the currents or, equivalently, the electromagnetic fields of the antenna's effective aperture, resulting in reversible changes in the antenna impedance and/or radiation properties [2]. Many techniques can be used to achieve the reconfiguration of an antenna. Most of these techniques employ switches, diodes or capacitors. Other techniques resort to mechanical alterations like a rotation or bending of a certain antenna part.

Reconfigurable antennas are mostly used on systems that require some type of change from one application to another. Reconfigurable antennas are used in multiple input multiple output (MIMO) situations, in cognitive radios, on laptops, in cellular phones and many other systems.

Graph models are widely used in computer science and in the development of networking algorithms [3]. Graphs also find applications in self-assembly robotics, where they are used to model the physics of particles by describing the outcomes of interactions among subsystems [4]. Herein we use graph models to optimize the structure of a reconfigurable antenna. We set graph modeling rules for the different types of switch-reconfigured antennas. We present several examples elaborating our modeling rules and optimization technique.

Manuscript received August 03, 2009; revised July 21, 2010; accepted August 20, 2010. Date of publication December 30, 2010; date of current version March 02, 2011.

J. Costantine is with the Electrical Engineering Department, California State University Fullerton, Fullerton, CA 92834 USA (e-mail: jcostantine@fullerton.edu).

S. al-Saffar is with the Knowledge Systems Group, Pacific National Laboratory, Seattle, WA 98115 USA.

C. G. Christodoulou and C. T. Abdallah are with the Electrical and Computer Engineering Department, University of New Mexico, Albuquerque, NM 87131 USA.

Color versions of one or more of the figures in this paper are available online at http://ieeexplore.ieee.org.

Digital Object Identifier 10.1109/TAP.2010.2103005

II. Introduction to Graphs

Graphs are symbolic representations of relationships between different components of a system. They are mathematical tools used to model complex systems in order to organize them and improve their status. In [5] the authors showed, briefly, that reconfigurable antennas can be modeled using graphs. A graph is defined as a collection of vertices that are connected by lines called edges. A graph can be either directed or undirected. The edges in a directed graph have a certain determined direction, while this is not the case in an undirected graph as shown in Fig. 1. Vertices may represent physical entities while the edges between them in the graph represent the presence of a function resulting from connecting these entities. If one is proposing a set of guidelines for antenna design, then a possible modeling rule may be to create an edge between two vertices whenever their physical connection results in a meaningful antenna function.

Edges may have weights associated with them, as shown in Fig. 1(b). These weights represent costs or benefits that are to be minimized or maximized. A path is an uninterrupted sequence of edges that are traveled in the same direction from an originating vertex to a destination vertex. The weight of a path is defined as the sum of the weights of its constituent edges. In some cases it is useful to find the shortest path connecting two vertices. This notion is used in graph algorithms in order to optimize a certain function. The shortest path distance in a non-weighted graph is defined as the minimum number of edges in any path from one vertex to another. If the graph is weighted, then the shortest path corresponds to the least sum of weights in a particular path. In a reconfigurable antenna design, a shorter path may mean a shorter current flow and thus a certain resonance associated with it. A longer path may denote a lower resonance frequency than that of a shorter path.

Adjacency-Matrix Representation: The adjacency-matrix representation of a graph G, assuming that the vertices are numbered $1, 2, \ldots, |\mathrm{V}|$ in some arbitrary manner, consists of a $|V| \times |V|$ matrix $A = (aij)$ such that [3]

$$a_{ij} = \begin{cases} 1 & if(i,j) \in E \\ 0 & Otherwise \end{cases} \\ where\ E\ is\ the\ set\ containing\ all\ edges. \tag{1}$$

The adjacency matrix of the graph shown in Fig. 1(a) is presented in the matrix A_1 below. The adjacency-matrix representation can also be used for weighted graphs. The corresponding weights in a graph are grouped into the adjacency matrix. For example, if $G = (V, E)$ is a weighted graph with edge-weight function $W(u, v)$ of the edge (u, v), then W is simply stored as the entry in row u and column v of the adjacency matrix. The lack of an edge is indicated by 0 in the adjacency matrix. The adjacency matrix of the graph shown in Fig. 1(b) is shown in the matrix A_2 as follows:

$$A_1 = \begin{bmatrix} 0 & 1 & 1 \\ 1 & 0 & 1 \\ 1 & 1 & 0 \end{bmatrix} \quad A_2 = \begin{bmatrix} 0 & 5 & 2 \\ 5 & 0 & 4 \\ 0 & 2 & 4 \end{bmatrix}.$$

Graph Modeling Rules: There are several ways to graph model reconfigurable antennas. Here we set some rules for graph modeling the different types of switch-reconfigured antennas. These rules are required for our optimization approach.

We set constraints for each rule in order to facilitate the graph modeling process. These constraints explain how to graph model each specific case of switch-reconfigured antennas. Herein an antenna is called a multi-part antenna if it is composed of an array of identical or different elements (triangular, rectangular...parts). Otherwise it is called a single-part antenna.

Rule 1: A multi-part antenna connected with switches is modeled as a weighted undirected graph. This graph consists of a vertex for each antenna part and connects those vertices with undirected weighted edges wherever the parts have a physical connection.

Constraints: The connection between two parts has a distinctive angular direction. The designer defines a reference axis that represents the direction that the majority of parts have in relation to each other or with a main part. The connections between the parts are represented by the edges. The edges' weights represent the angles that the connections make in relation to the reference axis. A weight $\mathrm{W} = 1$ is assigned to an edge representing a connection that has an angle $0°$ or $180°$ in relation to the reference axis. Otherwise a weight $\mathrm{W} = 2$ is assigned to the edge as shown in (2).

$$W_{ij} = P_{ij} \\ Where\ P_{ij} = \begin{cases} 1 & A_{ij} = 0° \ or\ 180° \\ 2 & Otherwise \end{cases} \tag{2}$$

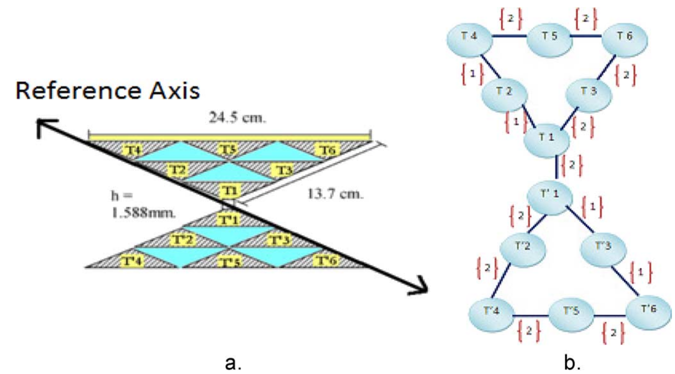

Fig. 2. The antenna structure in [6] with its graph model.

where $\mathrm{A_{ij}}$ represents the angle that the connection i,j form with the reference axis.

The removal or addition of a part in the reference axis direction affects one parameter in the antenna radiation characteristics (i.e. S11). The addition or removal of a part in a direction different from the reference axis direction affects many parameters (i.e., S11, radiation pattern and polarization); thus the bigger weight.

Example of rule 1: As an example, we take the antenna shown in Fig. 2(a) [6] and model it by a graph following rule 1. The basic antenna is a 130° balanced bowtie. A portion of the antenna corresponds to a two-iteration fractal Sierpinski dipole. The remaining elements are added (three on each side) to make the antenna a more generalized reconfigurable structure.

Following rule 1, the vertices in the graph model represent the triangles added. The edges connecting these vertices represent the connection of the corresponding triangles by MEMS switches. The graph modeling of this antenna is shown in Fig. 2(b). If a switch is activated to connect triangle T1 to triangle T′1 then an edge appears between the vertex T1 and the vertex T′1, as shown in Fig. 2(b). In this design the connections between T1 and T2, T2 and T4, T′1 and T′3, T′3 and T′6 are collinear with the reference axis. As a result, the edges representing these connections are weighted with $\mathrm{W} = 1$, and the other connections are weighted with $\mathrm{W} = 2$.

Rule 2: A single part antenna with switches bridging over slots is modeled as a non-weighted undirected graph. This graph consists of a vertex for every switch end-point and connects those vertices with non-weighted edges wherever switches are activated.

Constraints: In the case of switches bridging multiple slots in one antenna structure, the graph model takes into consideration one slot at a time.

Example of rule 2: As an example, we take the antenna shown in Fig. 3(a) [7]. This antenna is a triangular patch antenna with two slots. The authors suggested five switches to bridge each slot in order to achieve the required functions.

The graph modeling this antenna following rule 2 is shown in Fig. 3(b), where vertices represent the end points of each switch, and edges represent the connections between these end points. When switch 1 is activated, an edge appears between N1 and N′1 representing the two end-points of switch 1. The graph model in Fig. 3(b) represents each slot at a time. For example,

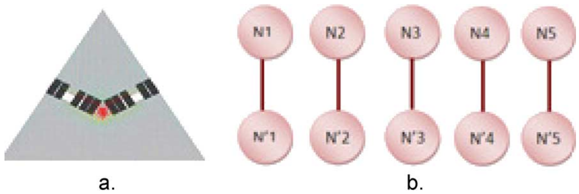

Fig. 3. The antenna structure in [7] with its graph model for all possible connections. a. Antenna structure; b. graph model.

N1 represents end-point 1 for switch 1 in slot 1 and end-point 1 for switch 1 in slot 2.

III. Structure Redundancy Optimization

An optimum reconfigurable antenna design yields the smallest number of redundant elements and achieves the functions required with great reliability. Our optimization approach allows the designer to identify the redundant parts in the design. These parts might be antenna topology parts that need to be removed, or electronic components such as switches. This technique removes redundancies from reconfigurable antenna structures to reduce costs and losses.

Herein, a part is defined as redundant if its presence gives the antenna more functions than required and its removal does not affect the antenna's desired performance. The removal of a part from the antenna structure may require a change in the dimensions of the remaining parts in order to preserve the antenna's original characteristics. That is, a redundant part can be removed as long as its removal will not affect the polarization status of the antenna in a reconfigurable return loss and reconfigurable polarization antenna.

For Multi-Part Switch-Reconfigured Antennas: The minimum number of edges present in any graph model according to rule 1 is equal to (N-1) and the maximum number is equal to N(N-1)/2. N represents the number of vertices in the graph model. In the case of a multi-part antenna and according to rule 1, N represents the different parts of the antenna. Eq. (3) shows the bounds of the number of edges NE in a graph model of this category

$$(N-1) \leq NE \leq \frac{N(N-1)}{2} = K_n \tag{3}$$

where $\mathrm{K_n}$ represents the maximum number of edges in a graph modeling a multi-part antenna. The number of unique paths (NUP) in such a graph model is always $\geq \mathrm{K_n}$ or else idle vertices are present; Keeping in mind that a path is a continuous sequence of edges that are traveled in the same direction from an originating vertex to a destination vertex. Then $\mathrm{K_n}$ is sufficient to be considered the necessary number of unique paths required to minimize redundancies. By decreasing the number of unique paths, the number of possible configurations is reduced, which results in reducing the number of vertices and removing redundant parts. Fig. 4 shows an example of how to identify the unique paths in a graph modeling a multi-part switch-reconfigured antenna.

Equation (4.b) shows the necessary number of available configurations (NAC) where the case of no connection is added.

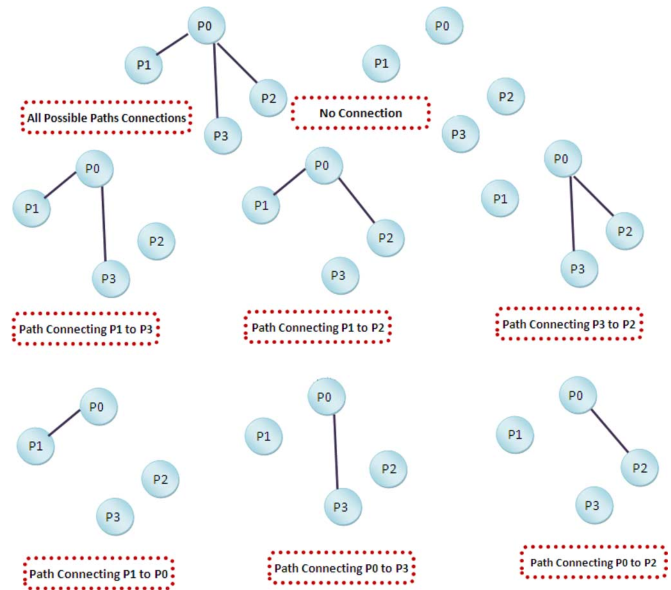

Fig. 4. An example of all possible unique paths in a given graph modeling a multi-part switch-reconfigured antenna.

Equation (4.c) is a direct derivation of (4.a) and (4.b) and represents the number of vertices required to achieve a certain number of configurations. The reconfigurable antenna may have more possible configurations than NAC for a given set of vertices; however, NAC represents the minimum number of antenna configurations that are necessary to achieve the maximum number of functions with the least number of components

$$NUP = \frac{N(N-1)}{2} \tag{4a}$$

$$NAC = NUP + 1. \tag{4b}$$

Using (4.a) and (4.b) we get

$$N^2 - N - 2 \times (NAC - 1) = 0 \Rightarrow$$

$$N = \left\lceil \frac{1 + \sqrt{1 + 8 \times (NAC - 1)}}{2} \right\rceil. \tag{4c}$$

For Single-Part Switch-Reconfigured Antennas: In the case of single-part antennas, vertices represent different end-points of switches. The number of vertices N in a graph modeling a single part switch-reconfigured antenna is twice the number of all possible edges. In this case, the number of possible unique paths is equal to the number of possible edges in the graph based on rule 2. Equation (5.a) represents the minimum number of available antenna configurations to achieve an efficient design. It is the number of possible edges in addition to the case where no connection exists. As in (4), the reconfigurable antenna might have more possible configurations than NAC for a given set of vertices. By rearranging (5.a), (5.b) is obtained and represents the number of vertices necessary to achieve a certain number of configurations

$$NAC = \frac{N}{2} + 1 \tag{5a}$$

$$N = 2 \times (NAC - 1). \tag{5b}$$

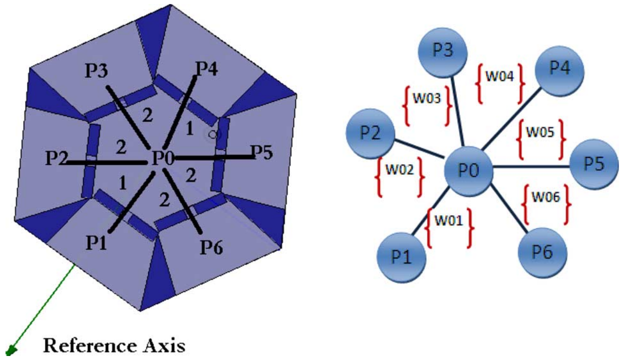

Fig. 5. Antenna in [8] and its graph model.

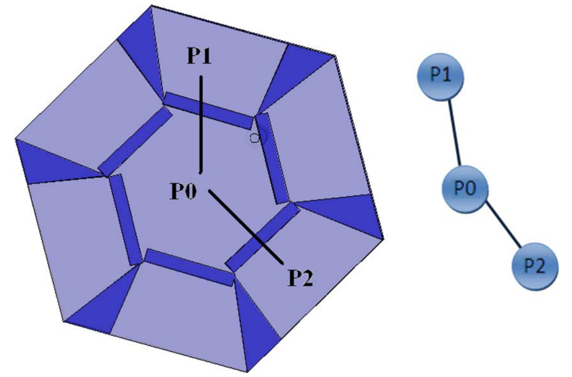

Fig. 6. The optimized structure with its graph model.

IV. Optimizing Redundancy in Multi-Part Switch-Reconfigured Antennas

Example IV.1: As an example we take the switch-reconfigured antenna shown in Fig. 5 [8]. This antenna is built out of a hexagonal main patch and six trapezoidal parts placed around it. The graph model of this antenna conforms to rule 1. The antenna is designed on an FR4 epoxy substrate ($\varepsilon_{\rm r} = 4.4$) with $\text{height} = 0.32\ \text{cm}$.

In addition to its original frequencies of operation, when all the switches are off, this antenna is required to have three more configurations that resonate as follows:

Configuration 1: 1 GHz, 3.5 GHz, 4.5 GHz;
Configuration 2: 3.5 GHz, 4.5 GHz, 5 GHz;
Configuration 3: 1 GHz, 2.5 GHz, 5 GHz;
Configuration 4 (All switches OFF): 3 GHz, 3.5 GHz, 4.5 GHz.

These frequencies represent practical applications such as WIMAX, WIFI, and GPS. This antenna was designed in [8] to have six switches connecting six sections to a main section. The application of (4.a), (b) to the graph model of this antenna shows that this antenna has at least 22 configurations, while just four configurations are required

$$\begin{aligned} NUP &= \frac{N(N-1)}{2} = \frac{7(7-1)}{2} = 21 \\ NAC &= NUP + 1 = 22. \end{aligned}$$

The application of (4.c) reveals that we need at most three vertices in the graph model to achieve these four required configurations

$$\begin{aligned} NAC &= 4 \\ N &= \left\lceil \frac{1+\sqrt{1+8\times(NAC-1)}}{2} \right\rceil \\ &= \left\lceil \frac{1+\sqrt{1+8\times(4-1)}}{2} \right\rceil = 3. \end{aligned}$$

To reduce the redundancy and complexity of this system and to minimize the design time and the number of simulations, the number of switches used has to be reduced to two. To preserve the radiation properties the general shape of the antenna as a six-armed hexagon cannot be disturbed, especially when all switches are OFF. The designer optimizes by simulations the placement of the two switches to achieve the required frequencies and configurations. The placements of these switches as well as the graph model of the optimized antenna are shown in Fig. 6. The simulated S11, the input reflection of this antenna, for all required configurations is shown in Fig. 7. By applying this technique, the design time has been reduced and, instead of determining the placement and topology of the antenna with six switches we need to do the work for only two. A comparison of the antenna's radiation patterns with redundant switches and the one without redundant elements at 4.517 GHz is shown in Fig. 8 for the x-y and y-z plane cuts.

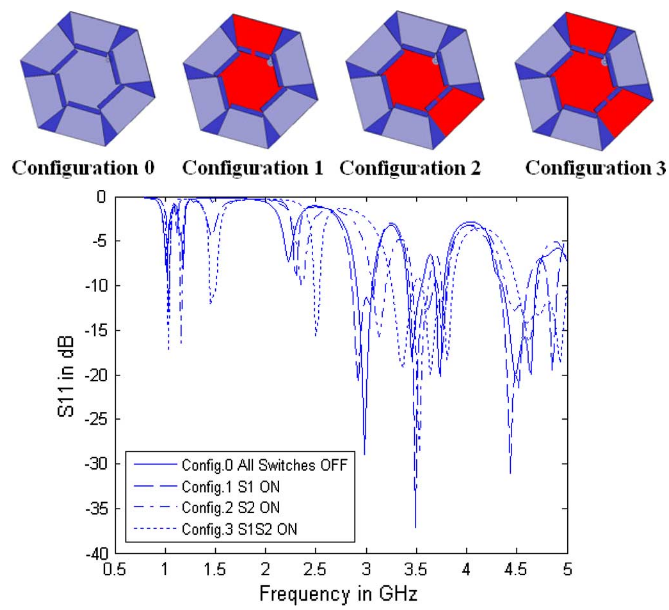

Fig. 7. The simulated input reflection (S11) plot for the required configurations.

Example IV.2: In this example the antenna [9] is a MEMS-reconfigurable pixel antenna that provides two functions: reconfiguration of its modes of radiation and reconfiguration of the operating frequency. The proposed antenna uses a 13 $\times$ 13 matrix of metallic pixels connected through MEMS switches in which circular patches of different radii are mapped.

Each metallic pixel has dimensions 1.2 $\times$ 1.2 mm, and the pixels are separated by 2 mm to provide enough space to allocate the MEMS switches and connecting lines. The MEMS switches around each pixel are activated or deactivated depending on the DC voltage that is supplied to the pixels. The DC connectivity

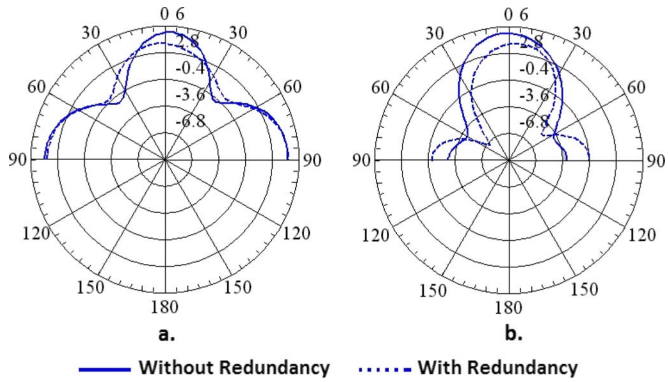

Fig. 8. Comparison of the antenna's simulated radiation patterns with and without redundant elements at 4.517 GHz for the x-y and y-z plane cuts.

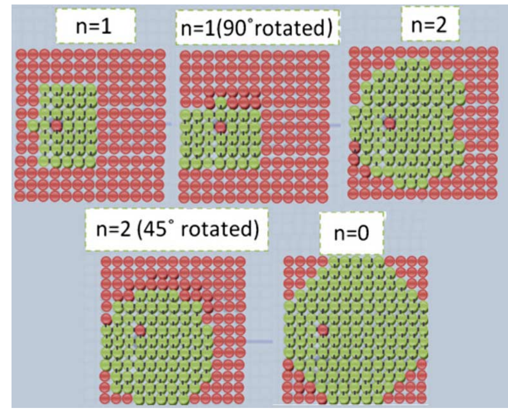

Fig. 9. Graph model of the required antenna configurations.

is provided through bias lines that connect the pixels to the back side of the substrate. In order to connect two metallic pixels, the voltage difference between them has to be around 30 V. The metallic pixels and the bias lines are connected through RF resistive lines made of Ni-chrome alloy. The substrate used is a quartz substrate that is 2 × 2 in, 1.575 mm thick and has a dielectric constant of 3.78. This antenna can generate five orthogonal radiation patterns at any frequency between 6 and 7 GHz. These patterns are those generated by the modes $\mathrm{n} = 1$, $\mathrm{n} = 2$ and $\mathrm{n} = 0$, all of them with $\phi_0 = 0°$, $\mathrm{n} = 1$ with $\phi_0 = 90°$, and $\mathrm{n} = 2$ with $\phi_0 = 45°$ [10]. At any fixed frequency between 6 and 7 GHz, five radiation states can be selected. The simulated flattened 3-D far field pattern for the $\mathrm{n} = 1$, $\mathrm{n} = 1$ with $\phi_0 = 90°$, $\mathrm{n} = 2$, $\mathrm{n} = 2$ with $\phi_0 = 45°$ and $\mathrm{n} = 0$ modes are shown in [10] This antenna exhibits frequency tuning as well as pattern/polarization diversity for fixed frequencies. The optimization approach introduced takes into consideration one reconfiguration function at a time, which in this case is the pattern/polarization. It is noted that five configurations are required. To graph model this antenna, the parts constituting its structure are treated as vertices. These vertices are connected by weighted undirected edges. The graph model of the antenna configurations required to achieve the five different modes of operation is shown in Fig. 9 and follows rule 1. Since only five configurations are required, applying (4.c) to this antenna gives us the number of parts required to achieve the desired configurations

$$N = \left\lceil \frac{1 + \sqrt{1 + 8 \times (NAC - 1)}}{2} \right\rceil = \left\lceil \frac{1 + \sqrt{1 + 8 \times (5 - 1)}}{2} \right\rceil = 4.$$

Only four configurations are required to achieve five antenna functions. The shape of the antenna with four parts will be very different from the one shown in Fig. 9 and needs to be simulated and investigated extensively. The antenna designer in [9] required a minimization of the number of switches used while keeping the same antenna topology. To preserve the same antenna topology, redundant connections have to be identified and redundant switches eliminated. By comparing the different graph models in Fig. 9, one notices that edges connect only certain vertices and the rest of the vertices remain idle in all five configurations. To identify the different sections of the antenna necessary to achieve the desired behavior, the adjacency matrix representation of the graph is used assuming the edges are not weighted. A part connected by an edge has a value 1, while a part that is not connected by any edge is represented by 0. The adjacency matrix representation for all possible configurations is shown in Table I. The matrices in Table I can be expressed as shown in (6)

$$A(\text{mode } n = 1) = S1 + S2 + S3 + S4 + S5 + S6 \tag{6a}$$

$$A(\text{mod } e\ n = 1\ Rotated\ 90°) = S1 + S2 + S3 + S8 + S12 + S13 + S14 \tag{6b}$$

$$A(\text{mod } e\ n = 2) = S1 + S2 + S3 + S4 + S5 + S6 + S7 + S8 + S9 + S10 + S15 + S17 + S27 \tag{6c}$$

$$A(\text{mod } e\ n = 2\ Rotated\ 45°) = S1 + S2 + S3 + S4 + S5 + S8 + S9 + S13 + S14 + S15 + S17 + S19 + S20 + S21 + S22 + S23 + S24 + S7 \tag{6d}$$

$$A(\text{mod } e\ n = 0) = \sum_{i=1}^{27} S_i \tag{6e}$$

where $\mathrm{S_{ij}}$ are defined in Table II.

The matrices in Table II can be translated into graphs representing each case. The corresponding graphs can be translated to antenna sections. These 27 antenna sections are shown in Fig. 10. Inside each section, the square patches are connected constantly, which eliminates the need for switches. Switches will be used only to connect the sections. Parts belonging to the same sections are always connected, and there is no need for switches inside each section. Some antenna parts are never connected, to achieve polarization diversity, and they are shown in black in Fig. 10. Using this technique, the number of switches is reduced by more than 100 from 312 to 166, while preserving the antenna topology. The reduction of the number of switches does not affect the radiation characteristics in [9] because the

TABLE I
ADJACENCY MATRIX REPRESENTATION FOR ALL POSSIBLE ANTENNA CONFIGURATIONS

Mode n=1	Mode n=1 With 90˚	Mode n=2	Mode n=2 with 45˚	Mode n=0
$A=\begin{bmatrix} 0&0&0&0&0&0&0&0&0&0&0&0&0\\ 0&0&0&0&0&0&0&0&0&0&0&0&0\\ 0&0&0&0&0&0&0&0&0&0&0&0&0\\ 0&0&1&1&1&1&1&0&0&0&0&0&0\\ 0&0&1&1&1&1&1&0&0&0&0&0&0\\ 0&0&1&1&1&1&1&0&0&0&0&0&0\\ 0&1&1&1&1&1&1&0&0&0&0&0&0\\ 0&0&1&1&1&1&1&0&0&0&0&0&0\\ 0&0&1&1&1&1&1&0&0&0&0&0&0\\ 0&0&1&1&1&1&1&0&0&0&0&0&0\\ 0&0&0&0&0&0&0&0&0&0&0&0&0\\ 0&0&0&0&0&0&0&0&0&0&0&0&0\\ 0&0&0&0&0&0&0&0&0&0&0&0&0 \end{bmatrix}$	$A=\begin{bmatrix} 0&0&0&0&0&0&0&0&0&0&0&0&0\\ 0&0&0&0&0&0&0&0&0&0&0&0&0\\ 0&0&0&0&0&0&0&0&0&0&0&0&0\\ 0&0&0&0&0&0&0&0&0&0&0&0&0\\ 0&0&0&1&0&0&0&0&0&0&0&0&0\\ 1&1&1&1&1&1&1&0&0&0&0&0&0\\ 1&1&1&1&1&1&1&0&0&0&0&0&0\\ 1&1&1&1&1&1&1&0&0&0&0&0&0\\ 1&1&1&1&1&1&1&0&0&0&0&0&0\\ 1&1&1&1&1&1&1&0&0&0&0&0&0\\ 0&0&0&0&0&0&0&0&0&0&0&0&0\\ 0&0&0&0&0&0&0&0&0&0&0&0&0\\ 0&0&0&0&0&0&0&0&0&0&0&0&0 \end{bmatrix}$	$A=\begin{bmatrix} 0&0&0&0&0&0&0&0&0&0&0&0&0\\ 0&0&0&0&1&1&1&0&0&0&0&0&0\\ 0&0&1&1&1&1&1&1&1&0&0&0&0\\ 0&1&1&1&1&1&1&1&1&1&0&0&0\\ 0&1&1&1&1&1&1&1&1&1&0&0&0\\ 1&1&1&1&1&1&1&1&1&0&0&0&0\\ 1&1&1&1&1&1&1&1&1&0&0&0&0\\ 1&1&1&1&1&1&1&1&1&0&0&0&0\\ 0&1&1&1&1&1&1&1&1&1&0&0&0\\ 0&1&1&1&1&1&1&1&1&1&0&0&0\\ 0&0&1&1&1&1&1&1&1&0&0&0&0\\ 0&0&0&0&1&1&1&0&0&0&0&0&0\\ 0&0&0&0&0&0&0&0&0&0&0&0&0 \end{bmatrix}$	$A=\begin{bmatrix} 0&0&0&0&0&0&0&0&0&0&0&0&0\\ 0&0&0&0&0&0&0&0&0&0&0&0&0\\ 0&0&0&0&0&0&0&0&0&0&0&0&0\\ 0&0&0&1&1&1&1&0&0&0&0&0&0\\ 0&1&1&1&1&1&1&1&1&0&0&0&0\\ 0&1&1&1&1&1&1&1&1&0&0&0&0\\ 1&1&1&1&1&1&1&1&1&1&0&0&0\\ 1&1&1&1&1&1&1&1&1&1&0&0&0\\ 1&1&1&1&1&1&1&1&1&1&0&0&0\\ 1&1&1&1&1&1&1&1&1&1&0&0&0\\ 0&1&1&1&1&1&1&1&1&1&0&0&0\\ 0&1&1&1&1&1&1&1&1&0&0&0&0\\ 0&0&0&1&1&1&1&1&0&0&0&0&0 \end{bmatrix}$	$A=\begin{bmatrix} 0&0&0&0&1&1&1&1&1&0&0&0&0\\ 0&0&0&1&1&1&1&1&1&1&0&0&0\\ 0&0&1&1&1&1&1&1&1&1&1&0&0\\ 0&1&1&1&1&1&1&1&1&1&1&1&0\\ 1&1&1&1&1&1&1&1&1&1&1&1&1\\ 1&1&1&1&1&1&1&1&1&1&1&1&1\\ 1&1&1&1&1&1&1&1&1&1&1&1&1\\ 1&1&1&1&1&1&1&1&1&1&1&1&1\\ 1&1&1&1&1&1&1&1&1&1&1&1&1\\ 0&1&1&1&1&1&1&1&1&1&1&1&0\\ 0&0&1&1&1&1&1&1&1&1&1&0&0\\ 0&0&0&1&1&1&1&1&1&1&0&0&0\\ 0&0&0&0&1&1&1&1&0&0&0&0&0 \end{bmatrix}$

TABLE II
THE MATRICES COMPOSING THE MATRICES OF TABLE I

$S1=\begin{cases} aij=1;\ i=6,7,8,9\ and\ j=3,4,5,6,7 \\ aij=0\quad Otherwise \end{cases}$	$S2=\begin{cases} aij=1;\ i=7\ and\ j=2 \\ aij=0\ Otherwise \end{cases}$	$S3=\begin{cases} aij=1;\ i=5\ and\ j=4 \\ aij=0\ Otherwise \end{cases}$
$S4=\begin{cases} aij=1;\ i=4\ and\ j=4,5,6,7 \\ or\ i=5\ and\ j=5,6,7 \\ aij=0\quad Otherwise \end{cases}$	$S5=\begin{cases} aij=1;\ i=5\ and\ j=3 \\ aij=0\ Otherwise \end{cases}$	$S6=\begin{cases} aij=1;\ i=4\ and\ j=3 \\ aij=0\ Otherwise \end{cases}$
$S7=\begin{cases} aij=1;\ i=2\ and\ j=5,6,7 \\ or\ i=3\ and\ j=3,4,5,6,7,8,9 \\ or\ i=3\ and\ j=3 \\ aij=0\quad Otherwise \end{cases}$	$S8=\begin{cases} aij=1;\quad i=6\ and\ j=2\ or\ i=7\ and\ j=1,2 \\ or\ i=8\ and\ j=1,2\ or\ i=9\ and\ j=2 \\ or\ i=10\ and\ j=2 \\ aij=0;\quad Otherwise \end{cases}$	$S9=\begin{cases} aij=1;\ i=5\ and\ j=2 \\ aij=0\ Otherwise \end{cases}$
$S10=\begin{cases} aij=1;\ i=4\ and\ j=3 \\ aij=0\ Otherwise \end{cases}$	$S11=\begin{cases} aij=1;\ i=5\ and\ j=1 \\ aij=0\ Otherwise \end{cases}$	$S12=\begin{cases} aij=1;\ i=6\ and\ j=1 \\ aij=0\ Otherwise \end{cases}$
$S13=\begin{cases} aij=1;\ i=9\ and\ j=1 \\ aij=0\ Otherwise \end{cases}$	$S14=\begin{cases} aij=1;\ i=10\ and\ j=1 \\ aij=0\ Otherwise \end{cases}$	$S15=\begin{cases} aij=1;\ j=8,9\ and\ i=5,6,7,8,9,10,11 \\ j=10\ and\ i=6,7,8,9,10 \\ aij=0\quad Otherwise \end{cases}$
$S16=\begin{cases} aij=1;\ i=4\ and\ j=8,9,10 \\ i=5\ and\ j=10 \\ aij=0\quad Otherwise \end{cases}$	$S17=\begin{cases} aij=1;\ i=11\ and\ j=3,4,5,6,7 \\ i=12\ and\ j=5,6,7 \\ aij=0\quad Otherwise \end{cases}$	$S18=\begin{cases} aij=1;\ i=12\ and\ j=4 \\ aij=0\ Otherwise \end{cases}$
$S19=\begin{cases} aij=1;\ i=13\ and\ j=5,6,7,8 \\ aij=0\ Otherwise \end{cases}$	$S20=\begin{cases} aij=1;\ i=13\ and\ j=4 \\ aij=0\ Otherwise \end{cases}$	$S21=\begin{cases} aij=1;\ i=11\ and\ j=2 \\ i=12\ and\ j=2,3 \\ aij=0\quad Otherwise \end{cases}$
$S22=\begin{cases} aij=1;\ i=11\ and\ j=10 \\ aij=0\ Otherwise \end{cases}$	$S23=\begin{cases} aij=1;\ i=7,8\ and\ j=10 \\ aij=0\ Otherwise \end{cases}$	$S24=\begin{cases} aij=1;\ i=12\ and\ j=8,9,10 \\ aij=0\ Otherwise \end{cases}$
$S25=\begin{cases} aij=1;\ i=1\ and\ j=5,6,7,8,9 \\ or\ i=2\ and\ j=8,9,10 \\ or\ i=3\ and\ j=10,11 \\ or\ i=4\ and\ j=11,12 \\ or\ i=5,6,7,8,9\ and\ j=11,12,13 \\ or\ i=11\ and\ j=11 \\ or\ i=6\ and\ j=10\ or\ i=10\ and\ j=11,12 \\ aij=0;\quad Otherwise \end{cases}$	$S26=\begin{cases} aij=1;\ i=2\ and\ j=4 \\ aij=0\ Otherwise \end{cases}$	$S27=\begin{cases} aij=1;\ i=6\ and\ j=2 \\ aij=0\ Otherwise \end{cases}$

topology has been preserved. Another example of reducing redundancies from a multi-part switch-reconfigured antenna can be found in [11]; where the antenna was optimally redesigned to maintain the same functionality and radiation characteristics.

V. OPTIMIZING REDUNDANCY IN SINGLE-PART SWITCH-RECONFIGURED ANTENNAS

Example V.1: In this example a single-part antenna is considered. This antenna [12], shown in Fig. 11 is a multi-band low-cost antenna that employs Koch fractal geometry. The antenna is fabricated on a 1.6 mm-thick FR4-epoxy substrate with dimensions 4 cm × 4.5 cm, is microstrip fed, and has a partial ground plane flushed with the feed line. A trapezoidal matching section connects the feed line to a U-Koch-slotted rectangular-Koch patch. The first-iterated Koch fractal geometry is used in the patch, and the U-slot is inserted to increase the antenna's electrical length for operation at lower frequency bands. Five pairs of RF MEMS are mounted across the slot, as shown in Fig. 11.

In [12] the symmetrically placed switches are activated two at a time to achieve the desired configurations. The first configuration, (10000), represents the activation of N1 and N′1 and the deactivation of the other eight switches. This configuration exhibits a narrow resonance at 1.9 GHz as well as a wide band operation between 2.7 and 6.6 GHz. The second configuration, (01000), represents the activation of N2 and N′2 while deactivating the other switches. This configuration achieves a resonance at 2.1 GHz and a wide band operation. from 2.4 to 6.7 GHz. The third configuration, (11111), represents the activation

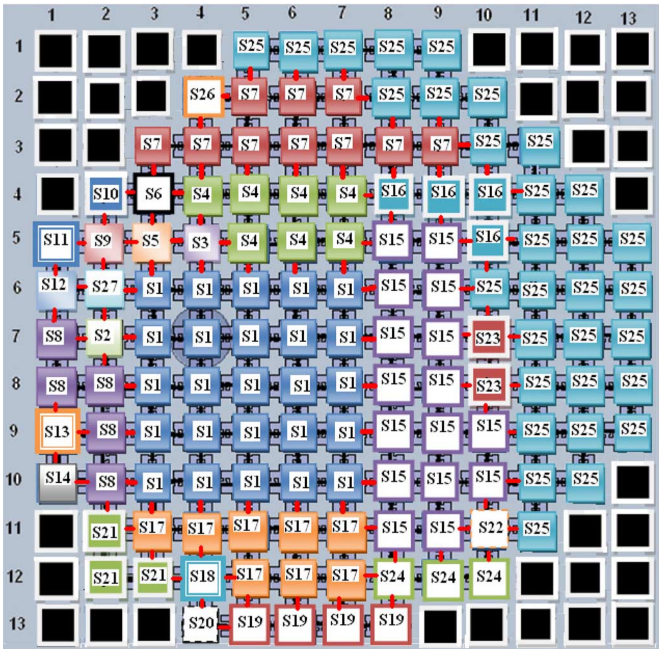

Fig. 10. The 27 antenna sections: red line indicating the presence of a switch and black line indicating the presence of a permanent connection (no need for a switch).

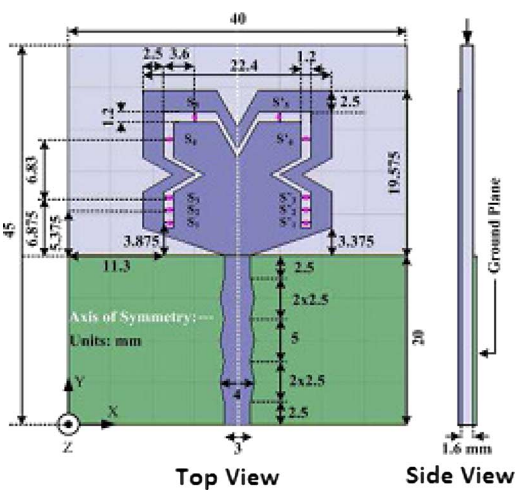

Fig. 11. The antenna topology in [12].

of all ten switches. This configuration achieves a wide band operation from 2.5 to 6.7 GHz. The graph model of the original structure is the same as the one shown in Fig. 3(b).

Investigating redundancies in this antenna structure, we can preserve the distinctive topology while removing redundant switches. Switches in this case have to be studied two at a time to preserve the antenna's operating modes.

In (5.a), N represents the end points of one side of the slots, so $N = 10$ in this case. Applying (5.a) to this antenna reveals that the minimum number of antenna configurations that can be achieved with five pairs of switches is six

$$NAC = \frac{10}{2} + 1 = 6.$$

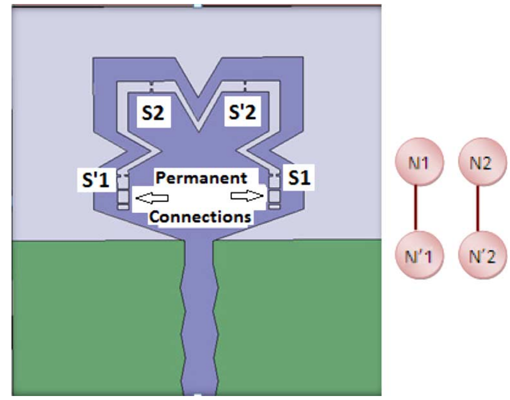

Fig. 12. Antenna with optimized number of switches and their positions, with the corresponding graph model.

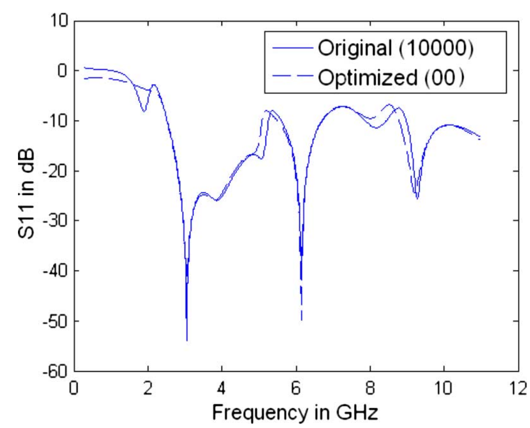

Fig. 13. Comparison of the input reflection of the original and the antenna with the optimized number of switches for case 1.

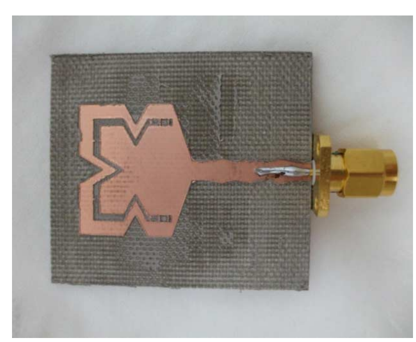

Fig. 14. The fabricated optimized prototype.

Since just three configurations are required, applying (5.b) reveals that only two switches are needed.

$$N = 2 \times (3 - 1) = 4.$$

The antenna topology with two switch positions is shown in Fig. 12 with the corresponding graph model. A comparison between the input reflection parameters of the original antenna and the antenna with the optimized number of switches is shown in Fig. 13 for the first required configurations. The fabricated prototype is shown in Fig. 14. A comparison of the analogies be-

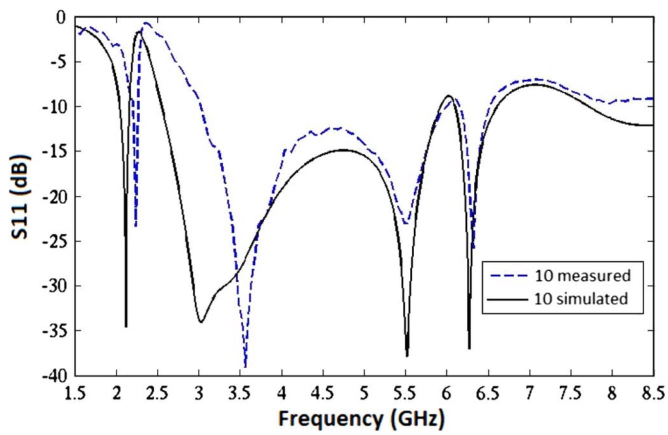

Fig. 15. Comparison of simulated and measured input reflection for the (10) optimized case.

tween the measured and simulated S11 for the (10) optimized case is shown in Fig. 15.

VI. Conclusion

In this paper, graphs are introduced as a modeling tool for reconfigurable antennas. Guidelines for graph modeling different types (multi-part and single part) of switch reconfigurable antennas are presented.

We also present a new methodology for removing redundancies from antenna structures. This approach is based on comparing the number of unique paths in a given graph with the number of the required antenna configurations. Equations are introduced for different types of switch reconfigurable antennas. In some cases redundant elements are simply removed from the antenna structures and in different cases a complete redesigning of the antenna is required. This optimization approach is an efficient tool for reducing costs and losses in reconfigurable antenna structures. Examples are given on multi and single-part switch reconfigured antennas, validating the discussed approach with simulations and measurement. Furthermore this easy approach does not replace the simulation in a design process however it reduces the number of iterations needed.

In addition, this paper proposes a complexity reduction approach while maintaining the desired multi-functional properties of a reconfigurable antenna, and facilitates the control of such antennas by using corresponding graph algorithms.

References

[1] J. T. Bernhard, *Reconfigurable Antennas*. San Rafael, CA: Morgan and Claypool, 2007.

[2] C. A. Balanis, *Modern Antenna Handbook*. Hoboken, NJ: Wiley, 2008.

[3] T. H. Cormen, C. E. Leiserson, R. L. Rivest, and C. Stein, *Introduction to Algorithms*, 2nd ed. Cambridge, MA: MIT press, 2001.

[4] E. Klavins, "Programmable self assembly," *IEEE Control Syst. Mag.*, vol. 27, no. 4, pp. 43–56, Aug. 2007.

[5] J. Costantine, C. G. Christodoulou, and S. E. Barbin, "Mapping reconfigurable antennas using graphs," in *Proc. NASA/ESA Conf. on Adaptive Hardware and Systems*, Jun. 2008, pp. 133–140.

[6] A. Patnaik, D. E. Anagnostou, C. G. Christodoulou, and J. C. Lyke, "Neurocomputational analysis of a multiband reconfigurable planar antenna," *IEEE Trans. Antennas Propag.*, vol. 53, no. 11, pp. 3453–3458, Nov. 2005.

[7] L. M. Feldner, C. D. Nordquist, and C. G. Christodoulou, "RFMEMS reconfigurable triangular patch antenna," in *Proc. IEEE AP/URSI Int. Symp.*, Jul. 2005, vol. 2A, pp. 388–391.

[8] J. Costantine, C. G. Christodoulou, and S. E. Barbin, "A new reconfigurable multi band patch antenna," in *Proc. IEEE IMOC Conf.*, Salvador, Brazil, Oct. 2007, pp. 75–78.

[9] A. Grau, L. Ming-Jer, J. Romeu, H. Jafarkhani, L. Jofre, and F. De Flaviis, "A multifunctional MEMS-reconfigurable pixel antenna for narrowband MIMO communications," in *Proc. IEEE Antennas and Propagation Society Int. Symp.*, Jun. 2007, pp. 489–492.

[10] R. G. Vaughan, "Two-port higher mode circular microstrip antennas," *IEEE Trans. Antennas Propag.*, vol. 36, no. 3, pp. 309–321, Mar. 1988.

[11] J. Costantine, C. G. Christodoulou, C. T. Abdallah, and S. E. Barbin, "Optimization and complexity reduction of switch-reconfigured antennas," *IEEE Antennas Wireless Propag. Lett.*, vol. 8, pp. 1072–1075, 2009.

[12] A. Ramadan, K. Y. Kabalan, A. El-Hajj, S. Khoury, and M. Al-Husseini, "A reconfigurable U-Koch microstrip antenna for wireless applications," *Progr. Electromagn. Res.*, vol. PIER 93, pp. 355–367, 2009.

Joseph Costantine (M'10) received the B.E. degree in electrical, electronics, computer, and communications engineering from the Lebanese University, in 2004, the M.E. degree in computer and communications engineering from the American University of Beirut, Beirut, Lebanon, in 2006, and the Ph.D. degree in electrical and computer engineering from the University of New Mexico, Albuquerque, in 2009.

In July 2010, he completed his Postdoctoral Fellowship in the Computer Engineering Department, University of New Mexico. Currently he is an Assistant Professor at the Electrical Engineering Department, California State University, Fullerton. He has also published many research papers and is a co-author of an upcoming book on reconfigurable antennas. His research interests are in the areas of reconfigurable systems and antennas, antennas in wireless communications, electromagnetic fields, RF Electronic Design and communication systems.

Dr. Costantine was awarded a 6-month research scholarship at Munich University of Technology (TUM) in 2006 as part of the TEMPUS program. He received many awards during his studies and career.

Sinan al-Saffar (M'10) received the M.S. degree in computer science from Arizona State University, in 1998, where his research focused on parallel and high performance computing, and the Ph.D. degree in computer engineering from the University of New Mexico, Albuquerque, in 2009. His Ph.D. work focused on applying semantic graphs and computation to subjective information valuation.

Previously, he spent a few years in Silicon Valley where his industry experience matured around parallel and high performance database systems, before returning to academia. Currently, he is a Senior Computer Scientist at the Pacific Northwest National Laboratory, Seattle, WA. His present research at PNNL combines data-intensive computing and semantic graph mining for automated knowledge discovery.

Dr. al-Saffar is an active member in the ACM and AAAS.

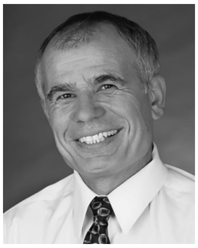

Christos G. Christodoulou (F'08) received the Ph.D. degree in electrical engineering from North Carolina State University, Raleigh, in 1985.

He served as a faculty member at the University of Central Florida, Orlando, from 1985 to 1998. In 1999, he joined the faculty of the Electrical and Computer Engineering Department, University of New Mexico, Albuquerque, where he served as the Chair of the department from 1999 to 2005. His research interests are in the areas of modeling of electromagnetic systems, FPGA reconfigurable systems, and smart RF/photonics. He has published over 350 papers in journals and conferences, has 12 book chapters and has coauthored four books.

Dr. Christodoulou is a Fellow of the IEEE and a member of Commission B of USNC/URSI. He is the winner of the John Kraus 2010 antenna award. He served as the General Chair of the IEEE Antennas and Propagation Society/URSI 1999 Symposium, Orlando, FL, as the Co-Chair of the IEEE 2000 Symposium on Antennas and Propagation for Wireless Communications, Waltham, MA, and the Co-Technical Chair for the IEEE Antennas and Propagation Society/URSI 2006 Symposium, Albuquerque. Currently, he is an Associate Editor for the IEEE TRANSACTIONS ON ANTENNAS AND PROPAGATION and the *IEEE Antennas and Propagation Magazine*. He was appointed as an IEEE AP-S Distinguished Lecturer (2007–now) and elected as the President for the Albuquerque IEEE Section. He served as an Associate Editor for the IEEE TRANSACTION ON ANTENNAS AND PROPAGATION for six years, was a Guest Editor for the *Applied Computational Electromagnetics Society (ACES)* Journal Special Issue on "Applications of Neural Networks in Electromagnetics," and was the Co-Editor of the IEEE TRANSACTION ON ANTENNAS AND PROPAGATION Special issue on "Synthesis and Optimization Techniques in Electromagnetics and Antenna System Design" (March 2007).

Chaouki T. Abdallah (SM'95) received the M.S. and Ph.D. degrees in electrical engineering from the Georgia Institute of Technology, Atlanta, in 1982 and 1988, respectively.

He joined the Electrical and Computer Engineering (ECE) Department, University of New Mexico, Albuquerque, where he is currently Professor and Department Chair. He was a Visiting Professor at the Universita Degli Studi di Roma, Tor Vergata, Rome, in 2005. He has published seven books (three as co-editor and four as coauthor) and more than 250 peer-reviewed papers. He conducts research and teaches courses in the general area of systems theory with focus on control, communications, and computing systems. His research has been funded by NSF, AFOSR, NRL, national laboratories, and by various companies.

Prof. Abdallah was the first recipient of ECE Department's Lawton Ellis Award for combined excellence in teaching, research, and student/community involvement. He also received the School of Engineering's senior research excellence award in 2004, and was the ECE Gardner Zemke Professor between 2002 and 2005. He served as Director of ECE's graduate program from 1999 through 2005. He has also been active in designing and implementing various international graduate programs with Latin American and European countries. In 1990, he was a co-founder of the ISTEC Consortium, which currently includes more than 150 universities in the US, Spain, and Latin America. He served as the General Chair of the 2008 CDC, which was held in Cancun, Mexico. He is a senior member of IEEE and a recipient of the IEEE Millennium medal.